REVERSE OSMOTIC CONCENTRATION OF AQUEOUS 2-BUTANONE (METHYL ETHYL KETONE), TETRAHYDROFURAN AND ETHYL ACETATE SOLUTIONS

MASAHIRO NIWA, HARUHIKO OHYA, EMIKO KUWAHARA AND YOUICHI NEGISHI

Department of Material Science and Chemical Engineering, Yokohama National University, Yokohama 240

Key Words: Membrane Separation, Reverse Osmosis, Composite Membrane, Cellulose Acetate Membrane, 2-Butanone, Tetrahydrofuran, Ethyl Acetate, Membrane Constant

Reverse osmotic concentration of aqueous MEK, THF and EAc solutions was carried out using five composite membranes (PEC-1000, FT-30 BW, FT-30 SW, NS-100 P1700, NS-100 P3500) and cellulose acetate membrane.

Separation of solute and permeation through the membranes were measured under the following conditions: concentration of MEK, 1–8.2 wt%; concentration of THF, 0.7–6.3 wt%; concentration of EAc, 0.8–3.9 wt%; operating pressure, 4–6 MPa. PEC-1000 gave the best solute separation for each system. Its separation was above 97.5% for MEK system, above 99% for THF system and above 97% for EAc system.

Membrane constants were calculated by the Spiegler-Kedem membrane transport model. The deviation from their model was corrected by compaction coefficients.

Energy and membrane area required to concentrate aqueous MEK, THF and EAc solutions using PEC-1000 were calculated.

Introduction

A large number of new reverse osmosis (abbr. RO) membranes have been developed in recent years. This development may open their new applications in separating organic solutes of molecular weights less than 100.

Feasibility studies of RO concentration have been carried out for the following solutes: alcohols,[8-10,17] carboxylic acids,[11,18] ketol compounds,[12] amines [13-15] and ε-caprolactam.[16]

Good water-soluble solvents such as 2-butanone (abbr. MEK), tetrahydrofuran (abbr. THF) and ethyl acetate (abbr. EAc) are widely used in industries related to surface coating. As for the recovery of these solvents, reverse osmotic concentration of their solutions by membrane seems more economical than distillation, and quite a few studies have been done. Using cellulose acetate (abbr. CA) membranes, Matsuura and Sourirajan[7] studied RO separation of MEK, THF and EAc of concentrations from 54 to 225 ppm. Rozell *et al.*[20] used NS-100 membrane for RO separation of MEK and THF of 1000 ppm concentration. Kurihara[5] studied RO separation of MEK and EAc of 4 wt% concentration.

In this study, RO concentration of three kinds of organic solutions was carried out using composite membranes and CA membranes. The dependency of rejection and flux on operating pressure (4–6 MPa) and feed concentration (1–8 wt%) was studied.

1. Experimental

1.1 Membranes

Three types of composite membranes were used for RO experiments: PEC-1000 supplied from Toray, FT-30 BW&SW from Filmtech, and NS-100 made in our laboratory on the basis of the method proposed by Cadotte.[1] Support UF membranes for NS-100 were from dimethylformamide solution of polysulfone (P1700 & P3500 from UCC).

Asymmetric CA membranes cast by Manjikian's method[6] were used as control after heat treatment at 90, 87 or 85°C.

1.2 Apparatus

The experimental apparatus was the same system described in the previous paper.[8]

1.3 Reagent and water

MEK, THF and EAc of guaranteed purity above 99%, above 99.5% and above 99%, respectively, from Wako Pure Chemical Industries, Ltd. were used as reagents without further prepurification. The permeate water through RO was used as process water after adding a slight amount of sodium thiosulfate.

1.4 Analysis

A total carbon analyzer, Toshiba-Beckman Model

Received June 20, 1987. Correspondence concerning this article should be addressed to M. Niwa. E. Kuwahara is now with Toray Industries Inc., Tokyo 103.

102, was used to measure the concentration of organic solutes.

1.5 Operation

Each membrane was characterized before and after the experiment for each system with ca. 3.5 wt% aqueous sodium chloride solution. **Table 1** shows the change of membrane characteristics. For MEK and THF systems, permeation flux after experiments for NS-100 was reduced to half the initial value. For the other membranes, the flux after experiments increased a little, while separation decreased.

For EAc system, in all membranes, both flux and separation declined.

Three levels of operating pressure were applied: 3.79–3.92, 4.77–4.9 and 5.75–5.88 MPa. A small difference in pressure at each level was caused by the pressure drop between the first cell and the last cell.

Separation and fluxes through the membranes were measured in the following ranges of concentrations; MEK: 1, 3, 5.5, 8.2 wt%; THF: 0.7, 1.8, 4.5, 6.3 wt%; EAc: 0.8, 1.7, 3.9 wt%. The experiments were done from low concentration system to high concentration, in order of concentration. The same membranes were used for a given system.

2. Transport Model

2.1 Physico-chemical data

The density and viscosity of aqueous MEK, THF and EAc solutions at 25°C were measured. The diffusion coefficient of each solute in water was estimated by the Wilke–Chang equation.[23] The osmotic pressure was estimated from Eq. (1)

$$\Pi(T) = -RT \ln a_w / v_w \tag{1}$$

where the activities of water of MEK and THF a_w were calculated by Wilson's equation using data presented by Othmer *et al.*[19] and Hirata,[3] respectively. a_w in EAc solution in the low concentration ranges was approximately 1.0,[2] whence osmotic ssure was estimated by van't Hoff's equation.

2.2 Transport equation

The relation between concentration of solute at the membrane (C_2) and concentration in the bulk solution (C_1) can be expressed by Eq. (2).[4]

$$(C_2 - C_3)/(C_1 - C_3) = \exp(J_v'/k) \tag{2}$$

Mass transfer coefficients on the surface of the membrane were estimated by Eq. (3), which was derived from data obtained with the same type of cell by Kimura and Sourirajan.[4]

$$N_{Sh} = 1.77 N_{Re}^{0.734} \cdot N_{Sc}^{0.33} \tag{3}$$

Various transport equations for reverse osmosis have been presented by different authors. To analyze the data obtained in this work, the following equations were chosen to calculate the permeation through a membrane using non-equilibrium thermodynamics derived by Staverman,[22] and Kedem and Katchalsky:[21]

$$J_v' = L_p'(\Delta P - \sigma \Delta \Pi) \tag{4}$$

$$J_v = L_p(\Delta P - \sigma \Delta \Pi) \tag{5}$$

$$J_s = \omega \Delta \Pi + (1-\sigma) J_v' \bar{C}_s \tag{6}$$

Spiegler and Kedem[21] divided the membrane into differential elements in the direction of its thickness and applied Eq. (4) in it in the form of a differential equation, integrating the equation to give the following form of intrinsic rejection.

$$R_{int} = (C_2 - C_3)/C_2 = \sigma(1-F)/(1-\sigma F) \tag{7}$$

where

$$F = \exp[-(1-\sigma)J_v'/\boldsymbol{P}] \tag{8}$$

$$\boldsymbol{P} = \omega RT \tag{9}$$

By extrapolating J_v' to infinite value, the value of R_{int} in Eq. (7) approaches reflection coefficient σ as the value of Eq. (8) approaches zero.

Table 1. Change of membrane characteristics

Membrane	System	Before exp. Salt rejection [%]	Before exp. Flux [mol·m^{-2}·s^{-1}]	After exp. Salt rejection [%]	After exp. Flux [mol·m^{-2}·s^{-1}]
PEC-1000	MEK	99.8	0.220	99.3	0.250
	THF	99.4	0.193	97.8	0.206
	EAc	99.9	0.197	99.6	0.175
FT-30 BW	MEK	97.9	0.184	95.6	0.215
	THF	96.8	0.555	97.1	0.239
	EAc	97.1	0.230	73.3	0.126
FT-30 SW	MEK	98.7	0.176	98.8	0.217
	THF	97.3	0.175	98.1	0.182
	EAc	98.2	0.182	93.6	0.119
NS-100 P. 3500	MEK	96.4	0.0512	95.9	0.0466
	THF	89.2	0.0899	91.2	0.0461
	EAc	95.7	0.0367	92.4	0.0278
NS-100 P. 1700	MEK	97.8	0.0763	98.0	0.0493
	THF	94.0	0.0544	95.1	0.0445
	EAc	99.2	0.0145	98.2	0.0136
CA (90)	MEK	99.0	0.0333	92.0	0.00356
	THF	99.4	0.0431	98.5	0.0396
	EAc	99.8	0.0361	96.6	0.00100

3. Results

3.1 PEC-1000

Figures 1, 2 and **3** show the relations of operating pressure to flux J_v and observed rejection R_{app} for MEK, THF and EAc systems, respectively. For MEK system, R_{app} was almost unchanged (better

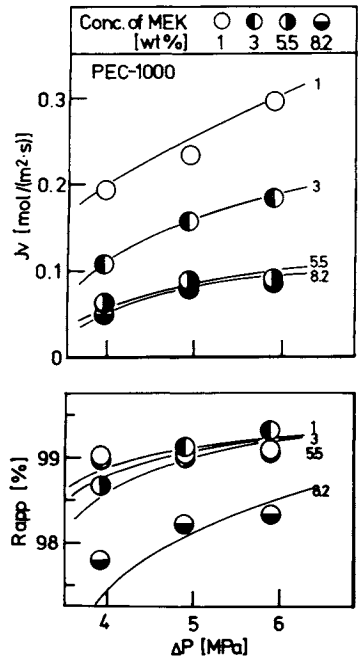

Fig. 1. Experimental data for PEC-1000 compared with calculated solution permeation flux and solute separation using Eqs. (2), (10) and (11) for MEK system

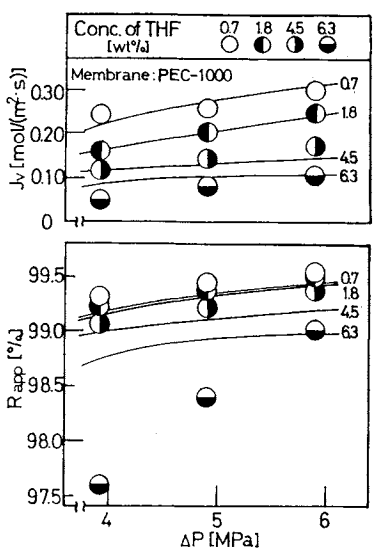

Fig. 2. Experimental data for PEC-1000 compared with calculated solution permeation flux and solute separation using Eqs. (2), (10) and (11) for THF system

than 98.5%) and was independent of operating pressure at the lower solute concentration, remaining above 97.5% even at a concentration of 8.2 wt%. Permeation flux was almost proportional to operating pressure and inversely proportional to concentration at the lower concentration. But at concentrations over 5.5 wt%, the flux seemed to remain almost constant. On the other hand, rejection remained unchanged up to a concentration of 5.5 wt% and decreased step by step at higher concentration. Both these phenomena were observed beyond the concentration of 5.5 wt%,

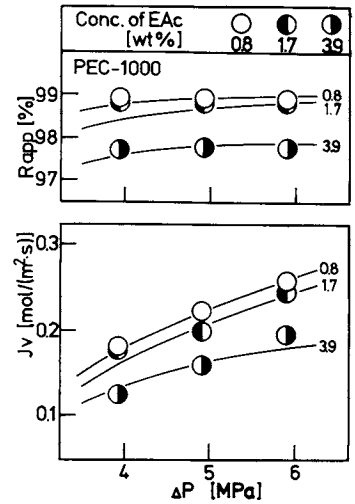

Fig. 3. Experimental data for PEC-1000 compared with calculated solution permeation flux and solute separation using Eqs. (2), (10) and (11) for EAc system

which seems to mean that the membrane starts to swell above a concentration of 5.5 wt%.

Experimental results for THF, as shown in Fig. 2, show a similar pattern. Similarly, the membrane starts to swell above 4.5 wt% concentration. It was compacted easily by applied pressure at 6.3 wt%. For EAc system, the swelling phenomenon was not observed, as shown in Fig. 3.

3.2 Other membranes

1) MEK system Concerning the results obtained with other membranes, FT-30 BW gave 70–90% rejection; NS-100 p3500, 80–95%; NS-100 p1700, 90–98%.

In the case of CA, the permeate flux was virtually zero. It gave 65–85% rejection at the concentration of 1 wt% and 40–60% at 3 wt%.

2) THF system Separation [%] and permeation flux [mol·m^{-2}s^{-1}] obtained were 40–80 and 0.1–0.8 with FT-30 BW; 70–90 and 0.05–0.3 with FT-30 SW; 92–98 and 0.01–0.09 with NS-100 P1700; 87–93 and 0.02–0.08 with NS-100 P3500; 50–60 and 0.02–0.06 with CA (90).

3) EAc system Separation [%] and permeation flux [mol·m^{-2}s^{-1}] obtained were 40–70 and 0.1–0.4 with FT-30 BW; 50–70 and 0.15–0.35 with FT-30 SW; 80–90 and 0.03–0.1 with NS-100 P1700; 90–97 and 0.02–0.05 with NS-100 P3500; less than 45 and less than 0.05 with CA (90); less than 40 and less than 0.15. In the case of CA, permeation flux was virtually zero at the concentration of 3.9 wt%.

4. Analysis of Data

4.1 Membrane constants

1) Reflection coefficient First of all, the intrinsic rejection R_{int} is given by correcting the effect of concentration polarization, using Eq. (2). The mass

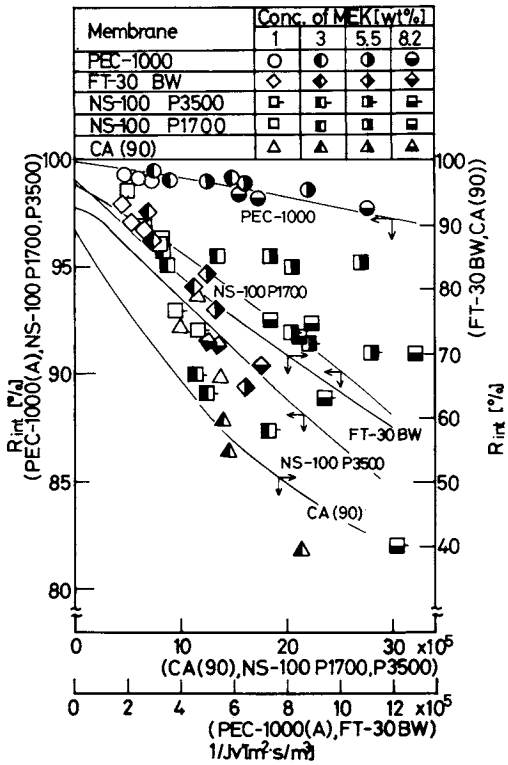

Fig. 4. Estimation of reflection coefficients by extrapolation to infinite permeation flux, using Eqs. (7) and (8) for MEK system

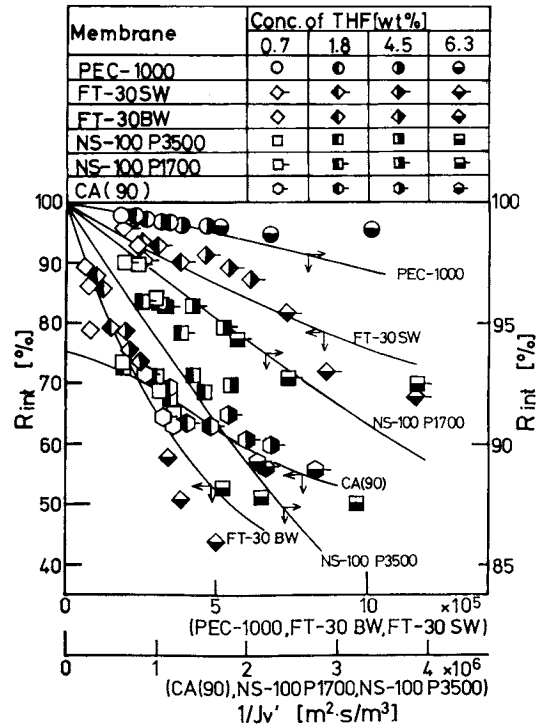

Fig. 5. Estimation of reflection coefficients by extrapolation to infinite permeation flux, using Eqs. (7) and (8) for THF system

transfer coefficient was calculated from Eq. (3).

The estimated values of R_{int} are plotted against $1/J_v'$ in **Figs. 4, 5** and **6**. Then the reflection coefficient is obtained by extrapolating the intrinsic rejection to infinite flux J_v' or zero of $1/J_v'$ on the ordinate axis in Figs. 4, 5 and 6 by the non-linear least square method with Eqs. (8) and (9), assuming $\boldsymbol{P}$ is constant. σ obtained with CA had minimum value of 0.88 and one with PEC-1000 had maximum value of 0.999 for MEK system. σ value obtained was 1.0 except that for CA, for THF system. σ value obtained was 1.0 with PEC and NS-100 P3500; 0.979 with NS-100 P1700; and 0.5–0.6 with two types of CA, for EAc system.

2) Hydraulic and solute permeability The hydraulic permeability and the solute permeability were estimated from Eqs. (5) and (6) and σ obtained above.

L_p^0 and ω^0 are obtained by extrapolating L_p and ω respectively for each solute concentration in feed to zero operating pressure. In these cases, it was difficult to find a definite relation of L_p and ω to operating pressure. Therefore, L_p^0 and ω^0 values used were the average of L_p and ω for each solute concentration, respectively.

The semi-logarithmic plot of L_p^0 and ω^0 against osmotic pressure of the solution on the surface of the membrane $\Pi(C_2)$ gives a linear relation as shown in **Figs. 7–12.**

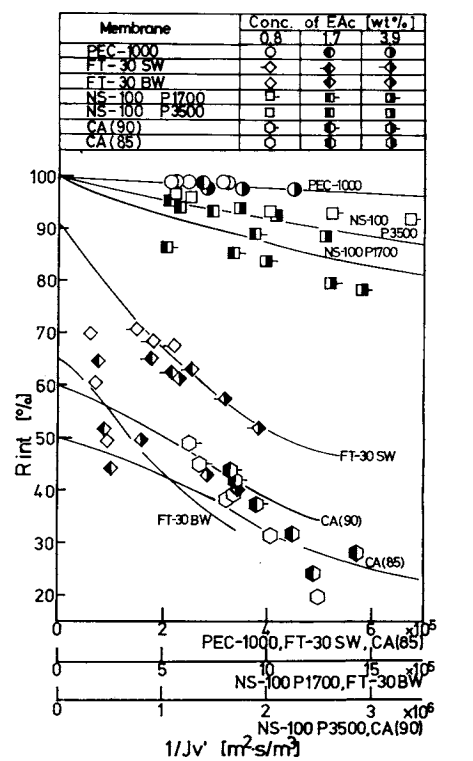

Fig. 6. Estimation of reflection coefficients by extrapolation to infinite permeation flux using Eqs. (7) and (8) for EAc system

The intercepts of the straight line give the values of L_{p0} and ω_0, and their slopes give compaction coefficients β_v and β_s, which are shown in **Table 2.**

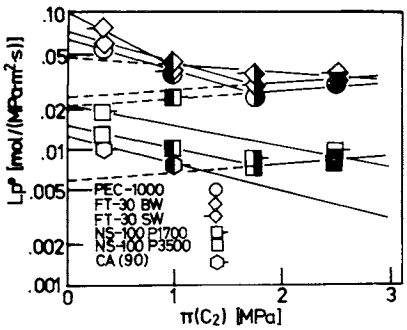

Fig. 7. Dependency of L_p^0 on osmotic pressure of solution on surface of membrane for MEK system (symbols are same as in Fig. 4)

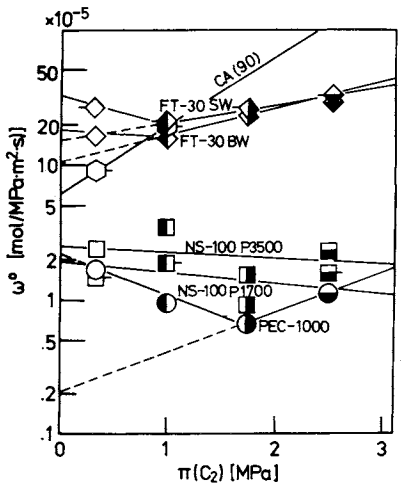

Fig. 8. Dependency of ω^0 on osmotic pressure of solution on surface of membrane for MEK system (symbols are same as in Fig. 4)

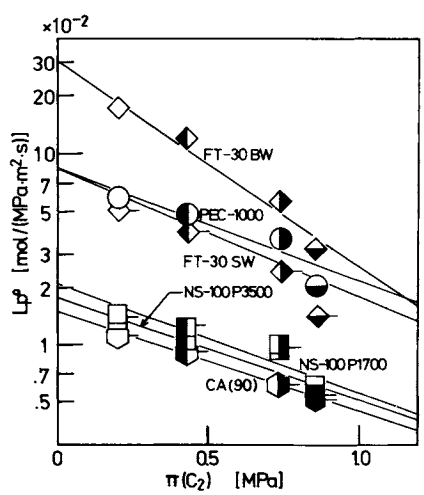

Fig. 9. Dependency of L_p^0 on osmotic pressure of solutions on surface of membrane for THF system (symbols are same as in Fig. 5)

The values of L_{p0} and ω_0 represent respectively the hydraulic permeability and solute permeability at zero operating pressure and solute concentration on the membrane.

In the case of MEK system, in Fig. 7, the values of

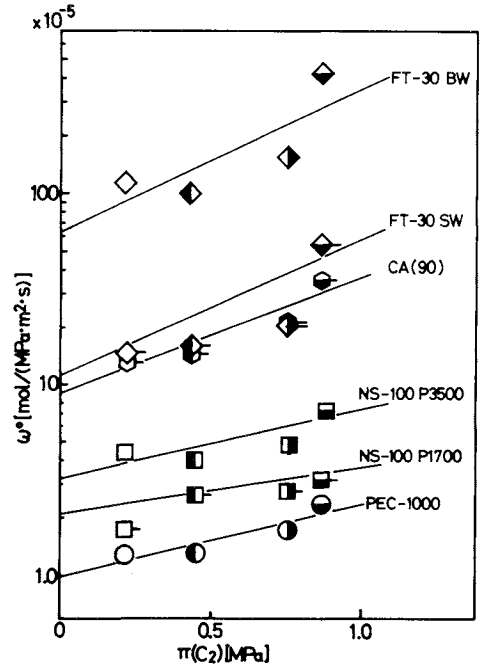

Fig. 10. Dependency of ω^0 on osmotic pressure of solution on surface of membrane for THF system (symbols are same as in Fig. 5)

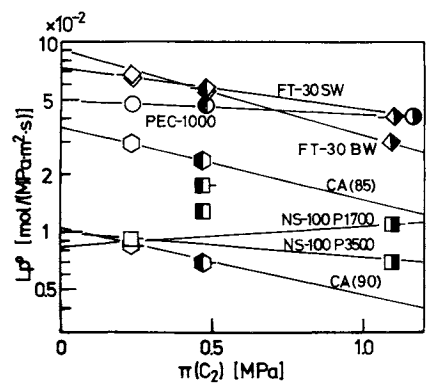

Fig. 11. Dependency of L_p^0 on osmotic pressure of solution on surface of membrane for EAc system (symbols are same as in Fig. 6)

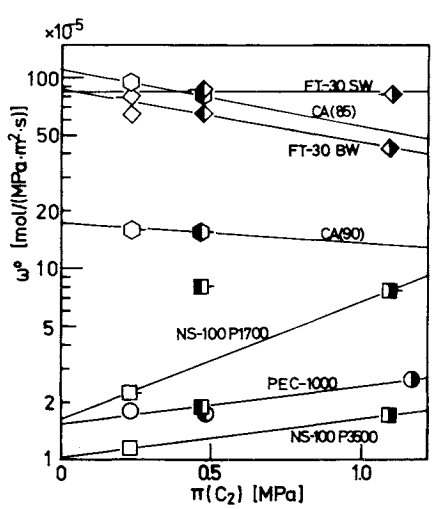

Fig. 12. Dependency of ω^0 on osmotic pressure of solution on surface of membrane for EAc system (symbols are same as in Fig. 6)

Table 2. Membrane constants

System	Membrane	Bulk conc. C_1 [wt%]	σ [—]	$L_{p0}\times 10^2$ 1 / $m^2\cdot MPa\cdot s$	$\omega_0\times 10^5$ 1 / $m^2\cdot MPa\cdot s$	β_v 1 / MPa	β_s 1 / MPa
MEK	PEC-1000	<5.5	0.999	6.60	2.05	0.539	0.679
		≧5.5	0.999	2.06	0.316	−0.158	−0.500
MEK	FT-30 BW	<3	0.970	6.90	18.0	0.496	0.870
		≧3	0.970	6.90	10.9	0.496	−0.462
		≧5.5	0.970	2.50	10.9	−0.080	−0.462
MEK	FT-30 SW	<3	0.985	9.30	33.0	0.949	0.278
		≧3	0.985	4.80	15.2	0.196	−0.332
MEK	NS-100 p3500	<5.5	0.977	1.49	2.56	0.389	0.086
		≧5.5	0.977	0.630	2.56	−0.114	0.086
MEK	NS-100 p1700		0.988	2.11	1.91	0.355	0.171
MEK	CA (90)		0.880	1.23	6.50	0.455	−1.1
THF	PEC-1000		1.0	8.35	0.980	1.41	−0.866
THF	FT-30 BW		1.0	30.8	61.7	2.51	−1.73
THF	FT-30 SW		1.0	8.53	11.2	1.60	−1.66
THF	NS-100 p3500		1.0	1.74	3.24	1.25	−0.842
THF	NS-100 p1700		1.0	2.08	1.61	1.35	−0.853
THF	CA (90)		0.754	1.49	9.03	1.19	−1.38
EAc	PEC-1000		1.0	4.98	1.54	0.163	−0.464
EAc	FT-30 BW		0.653	9.15	88.8	1.03	0.662
EAc	FT-30 SW		0.907	7.2	82.8	0.470	0
EAc	NS-100 p3500		1.0	1.00	1.04	0.324	−0.491
EAc	NS-100 p1700		0.979	0.850	1.63	−0.256	−0.141
EAc	CA (90)		0.602	1.06	17.6	0.894	0.235

L_p^0 decrease to an osmotic pressure of around 1.7 MPa and then slightly increase above that osmotic pressure. This result may mean that the membrane compacted, induced by solutes, up to around 1.7 MPa and then tended to swell around that pressure.

In the case of MEK system, solute permeabilities ω^0 with CA and NS membranes decreased monotonously with increasing $\Pi(C_2)$, those for PEC decreased to around 1.7 MPa and increased above that osmotic pressure and those for FT membranes declined with increasing osmotic pressure up to 0.85 MPa (in the case of L_p^0 decreasing around 1.7 MPa), as shown in Fig. 8.

In the case of THF system, the value of L_p^0 decreased with increasing osmotic pressure of solution on the surface of the membrane. FT-30 was superior in L_{p0}, on the other hand, and with CA was the smallest, as shown in Fig. 9.

Estimated ω^0 increased with increasing $\Pi(C_2)$ in contrast to the case for hydraulic permeability L_p^0. PEC-1000 gave the best solute separation, exhibiting the smallest ω_0. Conversely, CA and FT-30 gave relatively low solute separation, exhibiting large ω_0.

In the case of EAc system, as shown in Fig. 11, PEC and FT gave large flux and exhibited large hydraulic permeability constants L_{p0} of 0.05–0.09. Further, CA showed the smallest value.

ω^0 obtained with PEC and NS-100 increased with increasing EAc concentration in feed, while with the others its value declined with increasing concentration of solute.

4.2 Engineering model

Deviation from the model above is corrected by the compaction coefficients. Permeate flux J_v and solute permeate flux J_s can be described by Eqs. (10) and (11), respectively.

$$J_v = L_{p0}\exp(-\beta_v\Pi(C_2))(\Delta P-\sigma\Delta\Pi) \quad (10)$$

$$J_s = \omega_0\exp(-\beta_s\Pi(C_2))\Delta\Pi+(1-\sigma)J_v'\bar{C}_s \quad (11)$$

Permeate flux J_v and rejection R_{app}, estimated[5] from Eqs. (2), (10), (11) and the estimated membrane constants are shown as solid lines in Figs. 1, 2 and 3.

The solid lines generally agree with the plots.

5. Energy and Membrane Area Required

In **Fig. 13** is shown the calculated energy and membrane area required to concentrate MEK solution from 0.48 wt% to 3.05 wt% or 4.87 wt%.[9]

The calculated results in Fig. 13 show that the energy per kilogram of concentrated MEK is proportional to operating pressure and depends slightly on the final concentration and concentration polarization. It is found to be approximately 0.4 kWh/kg-MEK at $\Delta P=6$ MPa.

It is seen that the membrane area required is

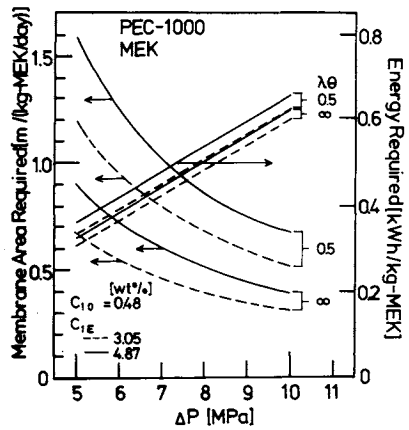

Fig. 13. Membrane area and energy required using PEC-1000 for MEK system

inversely proportional to operating pressure, depending on the final concentration and concentration polarization. Membrane area required when concentration polarization is neglected ($\lambda\theta=\infty$) is 75% smaller than that when concentration polarization is strong ($\lambda\theta=0.5$).

The calculated energy and membrane area required using PEC-1000 to concentrate THF and EAc solutions from 0.48 wt% to 3.05 wt% at $\Delta P=6$ MPa, when the concentration polarization is neglected, are 0.4 m^2/(kg-THF/day) and 0.35 kWh/kg-THF; and 0.4 m^2/(kg-EAc/day) and 0.5 kWh/kg-EAc, respectively.

Conclusion

(1) PEC-1000 gives the best solute separation of above 98.5% for MEK system, better than 97.5% for THF system and better than 97.5% for EAc system.

FT membranes are superior in flux but not so good as CA regarding rejection of organic solutes.

(2) Rejection and permeation fluxes decrease with increasing concentration of solute in feed. However, above a certain concentration of solute, it is observed that rejection decreases significantly and depends considerably on the applied pressure, and that permeation fluxes remain about constant.

These phenomena seem to mean that membrane compacts are induced by solute up to a certain concentration of solute and start to swell above that concentration.

(3) Using PEC-1000, at $\Delta P=6$ MPa, when the concentration polarization is neglected, the energy and the membrane area required to concentrate. MEK solution from 0.48 wt% to 3.05 wt% are approximately 0.55 m^2/(kg-MEK/day) and 0.4 kWh/kg-MEK; for concentration of THF solution from 0.48 wt% to 3.05 wt% they were 0.4 m^2/(kg-THF/day) and 0.35 kWh/kg-THF; for concentration of EAc solution from 0.59 wt% to 4.81 wt% they were 0.4 m^2/(kg-EAc/day) and 0.5 kWh/kg-EAc.

Nomenclature

a_w	=	activity of water in solution	[—]
C	=	molar density	[mol/m^3]
C_i	=	molar concentration	[mol/m^3]
$\mathscr{D}$	=	diffusivity	[m^2/s]
F	=	quantity defined by Eq. (7)	[—]
J_i	=	molar flux	[mol/(m^2·s)]
J_v'	=	volume flux	[m^3/(m^2·s)]
k	=	mass transfer coefficient	[m/s]
L_p	=	hydraulic permeability	[mol/(m^2·MPa·s)] [mol/(m^2·Pa·s)]
L_p'	=	hydraulic permeability	[m^3/(m^2·MPa·s)]
N_{Re}	=	ud/ν	[—]
N_{Sc}	=	$\nu/\mathscr{D}$	[—]
N_{Sh}	=	$kd/\mathscr{D}$	[—]
P	=	pressure	[MPa]
$\boldsymbol{P}$	=	ωRT	[m/s]
R	=	gas constant	[J/(mol·K]
R	=	solute separation	[—]
R_{app}	=	separation $(C_1-C_3)/C_1$	[—]
R_{int}	=	separation $(C_2-C_3)/C_2$	[—]
T	=	temperature	[K, °C]
u	=	velocity of solution parallel to membrane	[m/s]
v_w	=	partial molar volume of water	
β_s	=	solute-induced compaction coefficient	[1/MPa]
β_v	=	solute-induced compaction coefficient	[1/MPa]
Δ	=	difference	
Π	=	osmotic pressure	[MPa]
σ	=	reflection coefficient	[—]
ω	=	solute permeability	[mol/(m^2·MPa·s)]
$\lambda\theta$	=	k/v_ω^* dimensionless mass transfer coefficient	[—]

⟨Superscripts⟩

0	=	at zero pressure difference
—	=	average

⟨Subscripts⟩

s	=	solute
v	=	solution
0	=	value extrapolated at infinitesimal concentration
1	=	bulk solution
2	=	membrane–solution interface
3	=	permeate

Literature Cited

1) Cadotte, J. E. and L. T. Rozelle: *OSW R&DP Rept.*, No. 927 (1972).
2) Garner, F. H., S. R. M. Ellis and C. J. Pearce: *Chem. Eng. Sci.*, **3**, 48 (1954).
3) Hirata, M., S. Ohe and K. Nagahama: "Vapor-Liquid Equilibrium Data Computed by Electronic Computer," p. 490, Kodansya-Scientific (1975).
4) Kimura, S. and S. Sourirajan: *AIChE J.*, **13**, 497 (1967).
5) Kurihara, M.: *Desalination*, **38**, 449 (1981).
6) Manjikian, S.: *IEC PRD*, **6**, 23 (1967).
7) Matsuura, T. and S. Sourirajan: *J. Appl. Polym. Sci.*, **16**, 1663 (1972).
8) Ohya, H., E. Kazama and Y. Negishi: *Kagaku Kogaku Ronbunsyu*, **8**, 144 (1982).
9) Ohya, H.: *Kagaku Kogaku Ronbunshu*, **9**, 154 (1983).

10) Ohya, H., M, Okada, K. Okuno and Y. Negishi: *Maku*, **9**, 285 (1984).
11) Ohya, H., M. Niwa, K. Matsumoto, T. Osada, Y. Baba and A. Komura: *Maku*, **10**, 121 (1985).
12) Ohya, H., M. Niwa, M. Okada, K. Okuno, Y. Negishi, K. Matsumoto: *Maku*, **11**, 115 (1986).
13) Ohya, H., M. Okada, K. Okuno and Y. Negishi: *Maku*, **10**, 371 (1985).
14) Ohya, H., M. Okada, K. Okuno, Y. Negishi and M. Niwa: *Maku*, **10**, 313 (1985).
15) Ohya, H., E. Kuwahara, Y. Ishizu, M. Niwa, Y. Negishi and K. Matsumoto: *Maku*, **10**, 187 (1985).
16) Ohya, H., J. Taga, M. Okada, H. Yaguchi, T. Osada, Y. Baba and A. Komura: *Maku*, **8**, 171 (1983).
17) Osada, T., Y. Baba, S. Komura, Y. Ishizu and H. Ohya: *Maku*, **9**, 55 (1984).
18) Osada, T., Y. Baba, S. Komura, Y. Ishizu and H. Ohya: *Maku*, **9**, 285 (1984).
19) Othmer, O. F. and R. F. Benenati: *Ind. Eng. Chem.*, **37**, 299 (1945).
20) Rozelle, L. T., J. E. Cadotte and K. E.: Cabian "Reverse Osmosis Synth. Membrn.," p. 249 (1977).
21) Spiegler, K. S. and O. Kedem: *Desalination*, **1**, 311 (1966).
22) Staverman, A. J.: *Rec. Trav. Chim.*, **70**, 344 (1951).
23) Wilke, C. R. and P. Chang: *AIChE J.*, **1**, 264 (1955).

BUBBLE SIZE AND FREQUENCY IN GAS FLUIDIZED BEDS

JEONG H. CHOI AND JAE E. SON
Korea Institute of Energy and Resources, Dae Jeon, Korea
SANG D. KIM
Department of Chemical Engineering, Korea Advanced Institute of Science and Technology, Seoul 131, Korea

Key Words: Bubble Size, Bubble Frequency, Bubble Velocity, Fluidized Bed

A theoretical model for mean bubble size and frequency based on the collision theory with random spatial bubble distribution in freely bubbling gas-fluidized beds was developed. A hemispherical bubble velocity diagram was constructed to determine the average bubble collision frequency. The resulting theoretical equation for predicting bubble size is

$$(U-U_{mf})(D_b-D_{b0})+0.474\,g^{1/2}(D_b^{3/2}-D_{b0}^{3/2})=1.132(U-U_{mf})h$$

Bubble characteristics such as pierced bubble length, velocity and point frequency were measured in a square (30 × 30-cm) fluidized bed by means of an electroresistivity probe.

The gradient of bubble size increased linearly with bubble voidage. The bubble Froude number also increased along the bed height with bubble voidage. The bubble Froude number represents approximately a linear relationship with the average fractional change of square root of the static energy of bubble rise along the bed height. The present model of bubble size was found to represent well the data in the literature.

Introduction

In freely bubbling fluidized beds, the hydrodynamic behaviour is mainly governed by bubble properties such as bubble velocity, voidage, and frequency. This information is essential in the analysis of fluidized bed behaviour. Also, it may indicate whether a fluidized bed is operated in the slugging or bubbling state.

The bubble properties in three-dimensional beds have been measured by means of electrical probes, by photographing the bubbles which are erupting from the bed surface, and by an X-ray photographic method.

A semiempirical correlation for predicting the frontal diameter of a bubble has been presented by Rowe,[9] using a correlation of the number-density of bubbles determined by Rowe and Goldsmith.[12] Based on the literature data on bubble diameter, Darton *et al.*[3] have proposed a semiempirical correlation for predicting the equivalent spherical bubble diameter.

It has been reported that bubbles tend to rise along certain preferred paths and that coalescence may take place with a considerable lateral movement of bubbles which may be slow enough to determine the overall

Received June 22, 1987. Correspondence concerning this article should be addressed to S. D. Kim.